# A Model for Interlevel Coupling Noise in Multilevel Interconnect Structures

Martin Saint-Laurent[*], Zakaria Ajmal[†], Madhavan Swaminathan[†], and James D. Meindl[†]

[*] Intel Corporation, Austin, Texas, United States of America
[†] Georgia Institute of Technology, Atlanta, Georgia, United States of America

## Abstract

In multilevel interconnect structures, the interconnect layers are practically always perpendicular to each other. Because of the capacitive coupling between adjacent layers, the switching activity in one layer produces noise in the other. This paper analyses the interlevel coupling noise present at the far end of a victim line when a large number of perpendicular attackers are randomly switching. Each attacker is modeled as a Markov chain and the victim is modeled as an RLC transmission line. The result is a novel closed-form expression for the power spectral density of the interlevel coupling noise.

## Introduction

Interconnect noise has traditionally been and continues to be a significant issue for the design of high-performance microprocessors. Typically, it is addressed by determining the worst possible capacitive coupling noise that can be induced on a victim line by its parallel neighbors. In [1], the worst-case noise is simulated using an RC transmission line model that includes the timing of the attackers. In [2], inductance is taken into account and an expression for the peak crosstalk voltage between interconnects on the same layer is derived. In both cases, the conductors in layers adjacent to the victim's layer are assumed quiet. Each adjacent layer is treated as a virtual ground plane.

The problem with assuming that all interconnects perpendicular to the victim are quiet is that it underestimates the noise. Conversely, it is extremely pessimistic to assume that all conductors in the adjacent layers are simultaneously switching in the same direction. A better way to represent the interlevel coupling noise is to consider that the individual conductors in the adjacent layers are switching independently. A realistic noise model is sometimes very desirable, in particular for the design of clock distribution networks or the performance analysis of integrated antennas [5].

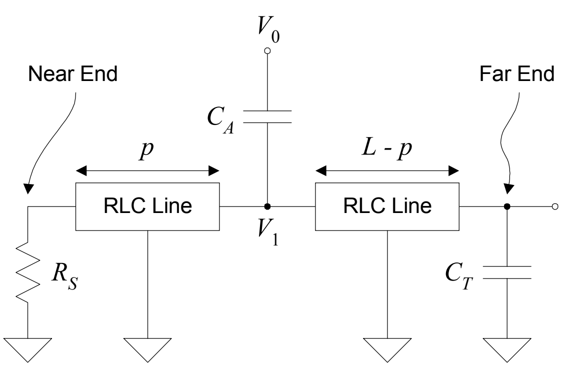

Fig. 2: Interconnect model.

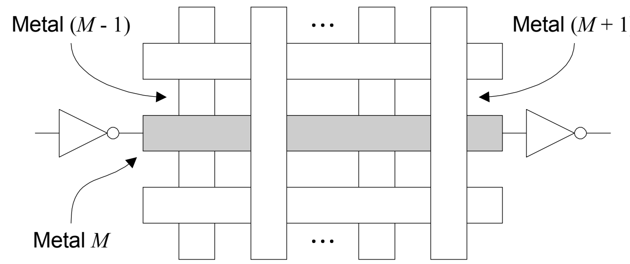

Fig. 1: Multilevel interconnect structure.

This paper analyses the interlevel coupling noise present at the far end of the victim line shown in Fig. 1 when a large number of perpendicular attackers are randomly switching. Each attacker is modeled as a Markov chain and the victim is modeled as an RLC transmission line. A closed-form expression for the power spectral density of the noise is derived for the first time. Finally, the noise characteristics are discussed for a typical 130-nm interconnect structure.

## Interlevel Coupling Noise Modeling

The effect of a particular attacker on the noise at the far end of the victim is modeled as shown in Fig. 2. The capacitance between the attacker and the victim is $C_A$. The source resistance $R_S$ represents the effective resistance of the circuit driving the victim and $C_T$ is the load capacitance that terminates it. The unit-length resistance, inductance, and capacitance of the victim line are $r$, $l$, and $c$. The length of the victim line is $L$ and $p$ is the position of the attacker. The pitch of each attacker (i.e. its width and space) is $\lambda$.

The victim line is modeled as a linear system with multiple inputs (one per attacker) and one output. The power spectral density of the noise at $V_2$ is obtained in three steps. First, the power spectral density of an individual attacker switching randomly at $V_0$ is analyzed. Then, its transfer function $H$ between $V_0$ and $V_2$ is derived. Since the system has multiple inputs, each attacker has its own transfer function. Given the power spectral density of the attacker at $V_0$ and the transfer function corresponding to its position, its

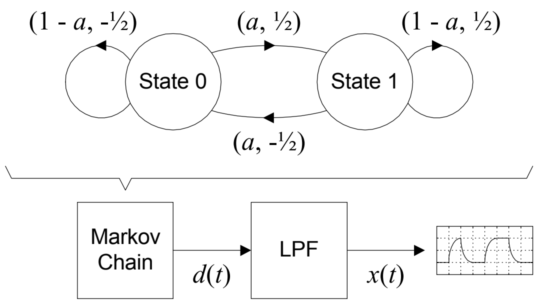


Fig. 3: Markov chain model for the switching activity of attackers.

contribution to the noise at $V_2$ is easy to compute. Finally, the total power spectral density of the noise at $V_2$ is determined by superposing the contribution of each individual attacker.

## Power Spectral Density for an Attacker Switching Randomly

During any given clock cycle, the probability that a particular attacker switches is its activity factor $a$. Its switching activity is modeled by the Markov chain producing $d(t)$ that is shown in Fig. 3. The shortest delay between state transitions is $T$. The power spectral density of $d(t)$ is [3]:

$$S_D(e^{j2\pi fT}) = \frac{a(1-a)}{1+(1-2a)^2 - 2(1-2a)\cos(2\pi fT)} \tag{1}$$

To produce the attacker waveform actually coupled to the victim, $d(t)$ is passed through a first-order low-pass filter $C$ having a gain $V$ and a time constant $\tau$. The power spectral density of the filter output $x(t)$ is given by [3]:

$$S_X(f) = S_D(e^{j2\pi fT})\left|C(j2\pi f)\right|^2 = S_D(e^{j2\pi fT})\frac{V^2}{(2\pi f\tau)^2+1} \tag{2}$$

It is worth noting that $x(t)$ is more realistic than a piecewise-linear waveform and that multiple switching can be modeled by making $T$ smaller than the actual clock cycle if $a$ is reduced accordingly.

## Interlevel Coupling Noise Transfer Function

The victim line has a propagation constant given by $\gamma = \sqrt{(r+sl)sc} = \alpha + j\beta$. Its characteristic impedance is:

$$Z_0 = \sqrt{\frac{r+sl}{sc}} = R_0 + jX_0 \tag{3}$$

The circuit for the victim line is equivalent to the circuit shown in Fig. 4. It is shown in [4] that:

$$\begin{aligned} Z_L &= Z_0\frac{R_S\cosh(\gamma p)+Z_0\sinh(\gamma p)}{R_S\sinh(\gamma p)+Z_0\cosh(\gamma p)} \\ Z_R &= Z_0\frac{\cosh(\gamma L-\gamma p)+Z_0 C_T s\sinh(\gamma L-\gamma p)}{\sinh(\gamma L-\gamma p)+Z_0 C_T s\cosh(\gamma L-\gamma p)} \end{aligned} \tag{4}$$

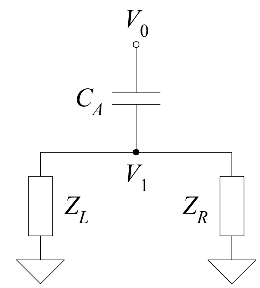


Fig. 4: Equivalent circuit for the victim line.

The transfer function between $V_0$ and $V_1$ is:

$$\frac{V_1}{V_0} = \frac{Z_L Z_R C_A s}{Z_L + Z_R + Z_L Z_R C_A s} \approx \frac{Z_L Z_R C_A s}{Z_L + Z_R} \tag{5}$$

The approximation is reasonable since $C_A$ is typically small enough to ensure that $|C_A\, 2\pi f| \ll 1$ below the cutoff frequency of the low-pass filter $C$. The transfer function from $V_1$ to $V_2$ is [4]:

$$\frac{V_2}{V_1} = \frac{1}{\cosh(\gamma L-\gamma p)+Z_0 C_T s\sinh(\gamma L-\gamma p)} \tag{6}$$

By definition, $H(s)$ is the product of (5) and (6). After some algebraic manipulations:

$$H(s) = \frac{Z_0 C_A s\left[R_S\cosh(\gamma p)+Z_0\sinh(\gamma p)\right]}{Z_0(R_S C_T s+1)\cosh(\gamma L)+(Z_0^2 C_T s+R_S)\sinh(\gamma L)} \tag{7}$$

The interlevel coupling transfer function varies according to $p$ and is different for each attacker. To make this dependence explicit, it is convenient to write $H(s, p) = F(s)G(s, p)$ where $G(s, p) = R_S\cosh(\gamma p) + Z_0\sinh(\gamma p)$.

## Power Spectral Density for the Far-End Noise

Let $y(t, p)$ be the far-end noise due to a single attacker located at position $p$. Its power spectral density is:

$$S_Y(f,p) = S_X(f)\left|H(j2\pi f, p)\right|^2 \tag{8}$$

Let P = {0, λ, 2λ, …, $L$} be the set containing the position of each attacker and let $n(t)$ be the total far-end noise. Its power spectral density is:

$$S_N(f) = \sum_{p\in P} S_Y(f,p) \approx S_X(f)\frac{1}{\lambda}\int_0^L \left|H(j2\pi f,p)\right|^2 dp \tag{9}$$

The discrete sum is approximated by an integral since the number of attackers is assumed very large. Therefore,

$$\begin{aligned} S_N(f) &= S_X(f)\left|F(j2\pi f)\right|^2 \frac{1}{\lambda}\int_0^L \left|G(j2\pi f,p)\right|^2 dp \\ &= S_X(f)\left|F(j2\pi f)\right|^2 \left|G_{eff}(j2\pi f)\right|^2 \end{aligned} \tag{10}$$

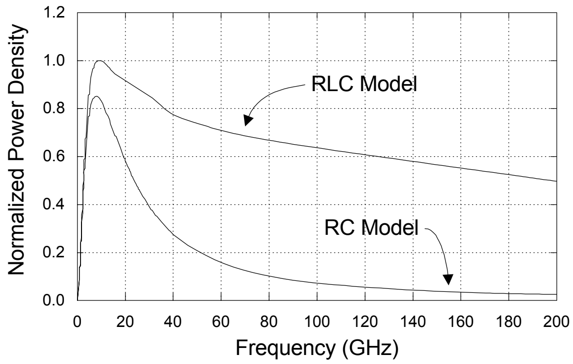


Fig. 5: Effect of inductance on the noise power spectral density envelope.

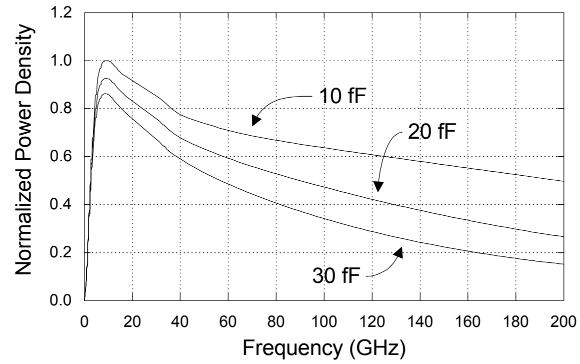


Fig. 6: Effect of the load capacitance on the noise power spectral density envelope.

where $G_{eff}(j2\pi f)$ is defined by the following equation:

$$\left|G_{eff}(j2\pi f)\right|^2 = \frac{1}{\lambda}\int_0^L \left|G(j2\pi f, p)\right|^2 dp \qquad (11)$$

By definition, $G_{eff}(j2\pi f)$ is a position-invariant effective transfer function. It produces an effect equivalent to the combined effect of the position-dependant transfer function of each attacker. It is tedious but straightforward to show that:

$$\begin{aligned}\left|G_{eff}(j2\pi f)\right|^2 &= \frac{\sinh^2(\alpha L)}{\lambda\alpha} R_0 R_S - \frac{\sin^2(\beta L)}{\lambda\beta} X_0 R_S \\ &+ \frac{\sinh(2\alpha L)}{4\lambda\alpha}(\left|Z_0\right|^2 + R_S^2) - \frac{\sin(2\beta L)}{4\lambda\beta}(\left|Z_0\right|^2 - R_S^2)\end{aligned} \qquad (12)$$

where $\alpha = \mathrm{Re}(\gamma)$, $\beta = \mathrm{Im}(\gamma)$, $R_0 = \mathrm{Re}(Z_0)$, and $X_0 = \mathrm{Im}(Z_0)$, as defined previously.

The closed-form expression for the power spectral density of the far-end noise is obtained by substituting (12) into (10). It is interesting to observe that $S_N(f)$ is proportional to $V^2 C_A^2 / \lambda$ at all frequencies. From (2), it is clear that $V^2$ measures the power of the attackers. The amount of power transferred to the victim line is also proportional to $|V_1/V_0|^2$ and therefore to $C_A^2$. Furthermore, the far-end noise is proportional to the number of attackers, which is inversely proportional to λ. Another interesting observation is that when $f = 0$ Hz, $|H(j2\pi f)| = 0$. In other words, the far-end noise has no DC component. When $f$ goes to infinity, $|H(j2\pi f)|$ goes to zero if the exact relationship between $V_0$ and $V_1$ is used in (5), but remains a positive constant if the approximate relationship is used instead. In practice, the actual behavior of $|H(j2\pi f)|$ is irrelevant because $|C(j2\pi f)\, H(j2\pi f)| = 0$ either way.

## Noise Characteristics for a Typical 130-nm Interconnect Structure

The power spectral density envelope of the noise at the far end of a 2000-µm victim line is shown in Fig. 5 for typical 130-nm technology parameters. The envelope is defined as $|C(j2\pi f)\, F(j2\pi f)\, G_{eff}(j2\pi f)|^2$. It only includes the electrical effects affecting the power spectral density of the noise. It does not include the properties of the data sequence $d(t)$ controlling the switching of each attacker. It is worth noting that the envelope is fairly flat and only reaches half of its peak at 200 GHz. Fig. 5 also demonstrates the importance of taking into account the inductance of the victim.

Fig. 6 shows how increasing the load terminating the victim line reduces the power of the interlevel coupling noise. When the load increases, the bandwidth of the victim line decreases and so does the bandwidth of the far-end noise. At high frequencies, most of the noise injected far from the end of the victim line is filtered out.

## Conclusions

The novel expression for the power spectral density of the interlevel coupling noise makes it possible to realistically model the switching activity of multilevel interconnect structures. Including the inductance of the victim is important to obtain an accurate model.

## References

[1] K. L. Shepard, V. Narayanan, and R. Rose, “Harmony: Static Noise Analysis of Deep Submicron Digital Integrated Circuits”, *IEEE Transactions on Computer-Aided Design of Integrated Circuits and Systems*, August 1999, pp. 1132-1150.

[2] J. A. Davis, and J. D. Meindl, “Compact Distributed RLC Interconnect Models—Part II: Coupled Line Transient Expressions and Peak Crosstalk in Multilevel Networks”, *IEEE Transactions on Electron Devices*, November 2000, pp. 2078-2087.

[3] E. A. Lee, and D. G. Messerschmitt, *Digital Communication*, Second Edition, Kluwer Academic Publishers, 1994, pp. 48-96.

[4] D. K. Cheng, *Fundamentals of Engineering Electromagnetics*, Addison-Wesley Publishing Company, 1993, pp. 336-385.

[5] B. Floyd, K. Kim, and K. O, “Wireless Interconnection in a CMOS IC with Integrated Antennas”, *IEEE International Solid-State Circuits Conference*, 2000, pp. 328-329.